THE
PHYSICS OF FLUIDS

VOLUME 5, NUMBER 11 NOVEMBER 1962

Structure of a Plane Shock Layer

H. W. LIEPMANN, R. NARASIMHA, AND M. T. CHAHINE
Graduate Aeronautical Laboratories and Jet Propulsion Laboratory, California Institute of Technology, Pasadena, California
(Received July 12, 1962)

The structure of a plane shock wave is discussed and the expected range of applicability of the Navier–Stokes equations within the shock layer is outlined. The shock profiles are computed using the Bhatnagar–Gross–Krook model of the Boltzmann equation and a uniformly converging iteration scheme starting from the Navier–Stokes solution. It is shown that the Navier–Stokes solution remains a good approximation in the high-pressure region of the shock layer up to approximately the point of maximum stress for all shock strengths. In the low-pressure region, the correct profiles deviate with increasing shock strength from the Navier–Stokes solution. The physical significance of the kinetic model used and the relation of the present study to previous theoretical and experimental work is discussed.

I. INTRODUCTION

THERE is little or no doubt that the shock structure in a monatomic, perfect gas is contained in the Boltzmann equation. To solve the complete Boltzmann equation for this simple problem is extremely involved and even if it could be done in this particular case the solution would serve only as a standard of comparison with approximate equations, simple enough to permit solutions for other configurations and easily extendable to other fluids. Indeed, the interest in the range of applicability of the Navier–Stokes equations rests largely with the fact that they are known to apply to a surprisingly large number of problems in liquids as well as in gases.

The shock-structure problem occupies a peculiar place in the study of the equations of motion because of its geometric simplicity and the absence of solid boundaries. Thus, the complication due to surface effects such as slip is removed. On the other hand, no reference length is introduced by the geometry and hence it is impossible to state *a priori* a simple condition for the existence of limiting cases like a free-molecular-flow or a Navier–Stokes regime. The applicability of a particular equation or solution has to be entirely judged by its internal consistency, its agreement with a possible future exact solution, or finally with experiment.

The present paper is intended to clarify the relation of the Navier–Stokes solution to the exact shock-layer profile and to define the region within the layer where deviation from the Navier–Stokes solution must occur, kinetic models have to be used, and upon which experiments should be concentrated. (For example, it will be shown that the so-called maximum slope thickness of the shock wave is given with sufficient accuracy for all shock strengths by the Navier–Stokes solution and hence does not present a suitable quantity to differentiate between the correct and the Navier–Stokes solution.)

To do this, we begin with an over-all discussion of simple but significant general features of the Navier–Stokes solution (Sec. II). In particular, we know that the Navier–Stokes equation must be correct for small values of the ratio of compression stress τ, say, and pressure p. Hence, we derive first an explicit relation for τ/p within the layer. It turns out that starting from the high-pressure side ("downstream") one can expect the Navier–Stokes equations to apply at least up to the region of maximum gradients; beyond this region, one can expect deviations which become progressively larger as the shock strength increases. To compute the complete shock profile an iterative method of solving the B–G–K (Bhatnagar, Gross, and Krook) model for the Boltzmann equation is used

starting from the known Navier–Stokes solution. The significance of the model is discussed first (Sec. III). In Sec. IV the method of iteration is described. The method depends in each step only on the lowest moments of the distribution function of the previous step and not on the detailed shape of the distribution function itself; hence, the iteration procedure differs essentially from the Chapman–Enskog expansion and converges rather rapidly. The results of the computations are discussed in Sec. V.

The iteration procedure reproduces the Navier–Stokes solution in the downstream (high-pressure)

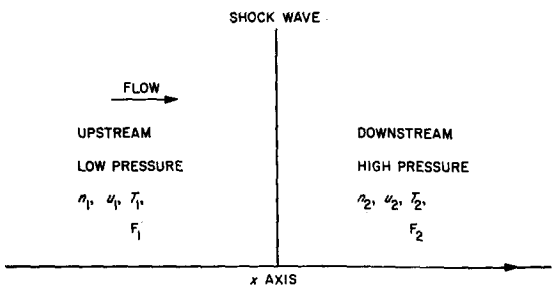

FIG. 1. Notation.

region of the layer but tends toward a very different profile in the upstream (low-pressure) region of the shock, completely in line with the expectation from the general discussion of the behavior of τ/p. In particular, the upstream end of the pressure and temperature distributions are much broader than the corresponding Navier–Stokes profiles.

We believe that the results of these computations give the shock structure qualitatively correctly and quantitatively very nearly so, since the B–G–K model can be shown to be correct in both the Navier–Stokes and the free-molecular limit and since the whole scheme fits in with some quite general over-all considerations.

In particular, no *a priori* decision whether to apply the Navier–Stokes equations of a kinetic model was made, but it was attempted to obtain a consistent approach from both sides. A brief discussion of the present work in relation to the extensive literature on the shock-layer problem is given in Sec. V. Useful surveys of the background of the problem of shock structure can be found in the articles by Hayes and Lighthill[1] and in Sherman and Talbot's paper.[2]

[1] W. D. Hayes, *Gasdynamic Discontinuities* (Princeton University Press, Princeton, New Jersey, 1960); M. J. Lighthill, in *Surveys in Mechanics*, edited by G. K. Batchelor and R. M. Davies (Cambridge University Press, New York, 1956).

[2] F. S. Sherman and L. Talbot, in *Rarefied Gas Dynamics*, edited by F. M. Devienne (Pergamon Press, New York, 1960).

II. NAVIER–STOKES SOLUTION: SOME SIGNIFICANT FEATURES AND ITS SELF-CONSISTENCY

We choose shock-fixed coordinates with the velocity u in the positive x direction (Fig. 1). The thermodynamic state is defined in terms of the enthalpy and entropy per unit mass h and s. The so-called total enthalpy $h + \frac{1}{2}u^2$ will be denoted by H. The viscous-stress tensor and the heat-flux vector each have only one component denoted by τ and q, respectively. All other symbols used are standard or will be defined as needed.

The state ahead of the shock layer, i.e., for $x \to -\infty$, will be denoted by (1), the downstream state $x \to +\infty$ by (2).

With this choice, the conservation equations can be written in the form

$$\rho u = \text{const} = m \quad \text{(say)}, \tag{2.1a}$$

$$m(u - u_1) + p - p_1 = \tau, \tag{2.1b}$$

$$m(H - H_1) = \tau u - q. \tag{2.1c}$$

Together with an equation of state, the system is complete. It is, however, sometimes interesting to use also an equation for the specific entropy, i.e.,

$$mT\frac{ds}{dx} = \frac{d}{dx}(\tau u - q) - u\frac{d\tau}{dx}. \tag{2.1d}$$

In the Navier–Stokes approximation,

$$\tau = \tilde{\mu}\frac{du}{dx}, \qquad q = -\frac{k}{c_p}\frac{dh}{dx},$$

where $\tilde{\mu}$ is related to the ordinary shear viscosity μ and bulk viscosity κ by

$$\tilde{\mu} = (4/3)\mu + \kappa.$$

$\tilde{\mu}$, the heat conductivity k, and the specific heat C_p are for a perfect gas, functions of the temperature or enthalpy only.

A Prandtl number $\tilde{\text{Pr}}$ is used, defined by

$$\tilde{\text{Pr}} = \tilde{\mu}c_p/\kappa.$$

$\tilde{\text{Pr}}$ is here more convenient to use than the usual definition of $\text{Pr} = \mu C_p/k$. For a monatomic gas, $\kappa = 0$ and they are simply related by $\tilde{\text{Pr}} = (4/3)\,\text{Pr}$. We will now derive a few very simple relations and estimates from Eqs. (2.1). These will be used to outline the general flow pattern within the shock layer and, in particular, to pinpoint the region within the layer where the Navier–Stokes equations are suspect.

A. Energy Integral

If $\tau u = q$, Eq. (2.1c) integrates immediately to $H = H_1 = \text{const}$. Within the Navier–Stokes

approximation, this solution corresponds to a Prandtl number $\tilde{\mathrm{Pr}} = 1$ and was already found by Becker[3] long ago. The Prandtl number of real gases is so close to unity that it is possible to derive easily an upper bound for the variation of H within the layer. From Eq. (2.1c), it follows that at the point where H has a stationary value $\Delta H = (H - H_1)_{\max}$ satisfies

$$\frac{\Delta H}{H_1} = \frac{\tilde{\mathrm{Pr}} - 1}{\tilde{\mathrm{Pr}}} \frac{\tau u}{m H_1}. \tag{2.2}$$

Since the right side of (2.2) involves the small parameter $\tilde{\mathrm{Pr}} - 1$ already, one can evaluate τu from the equation for $\tilde{\mathrm{Pr}} = 1$, i.e., using $H = \text{const}$. In particular, the maximum value of τu within the shock layer can be written down in the form

$$|\tau u|_{\max} = [(\gamma + 1)/2\gamma] m u_1^2 (1 - a^{*2}/u_1^2)^2, \tag{2.3}$$

where ν is the ratio of specific heats and a^* is a velocity of sound defined by

$$a^{*2} = [2(\gamma - 1)/(\gamma + 1)] H_1.$$

Consequently,

$$\frac{\Delta H}{H_1} < \frac{\tilde{\mathrm{Pr}} - 1}{\tilde{\mathrm{Pr}}} \frac{\gamma + 1}{8\gamma} \left(1 - \frac{a^{*2}}{u_1^2}\right)^2,$$

and since $(a^*/u_1)^2$ varies between 1 and $(\gamma-1)/(\gamma+1)$ only, we have

$$\Delta H/H_1 < (\tilde{\mathrm{Pr}} - 1)/\tilde{\mathrm{Pr}}\, 2\gamma(\gamma + 1). \tag{2.4}$$

For a monatomic gas, the Chapman–Enskog value for Pr is 8/9 and, hence,

$$\Delta H/H_1 < 0.014.$$

Hence, even for shock waves of infinite strength, H varies by less than 2% through the layer and the effect of this variation on the distribution of ρ, u, T, p, etc. should be insignificant for our purposes. This is borne out by a sample computation (cf. Fig. 2). Consequently the use of $H = \text{const}$ for the following remarks is justified. Indeed, one can state in general that small differences in the Prandtl number will have little effect on the shock-layer profiles. The characteristic gas parameters which determine the layer are γ and $\mu(T)$.

B. Stress Distribution

In the following, we will use the relation $H = H_1 = \text{const}$ and use a^* as the reference velocity, i.e., we will write $W = u/a^*$. It is also convenient to introduce $\lambda^2 = (\gamma + 1)/(\gamma - 1)$ to shorten the

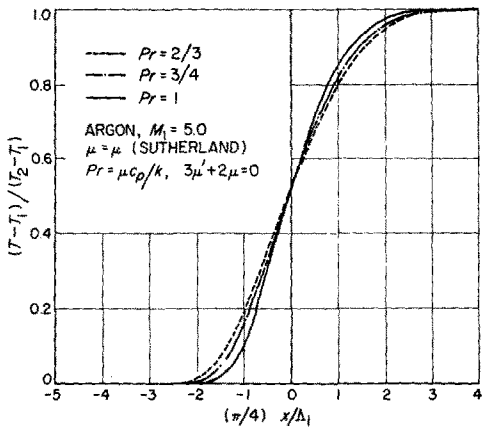

FIG. 2. Effect of Prandtl number on Navier–Stokes shock structure.

equations. From the conditions for a normal shock, we have[4]

$$W_1 W_2 = 1, \qquad 1 < W_1 \leq \lambda.$$

For simple gases, λ^2 is an integer, e.g., for a monatomic gas $\lambda^2 = 4$. W is related to the local Mach number $M = u/a$ by

$$W^2 = (\gamma + 1)M^2/[2 + (\gamma - 1)M^2].$$

From (2.1b) it follows easily that the maximum stress $\tau_{\max}$ occurs at the sonic point within the layer and, hence,

$$|\tau(W)|_{\max} = \frac{\lambda^2}{\lambda^2 + 1} m a^* \frac{(W_1 - 1)^2}{W_1} = \tau^* \quad \text{(say)}. \tag{2.5}$$

The maximum stress in a shock is reached, consequently, at a point ($W = 1$) near the high-density side of the layer. This simple result already

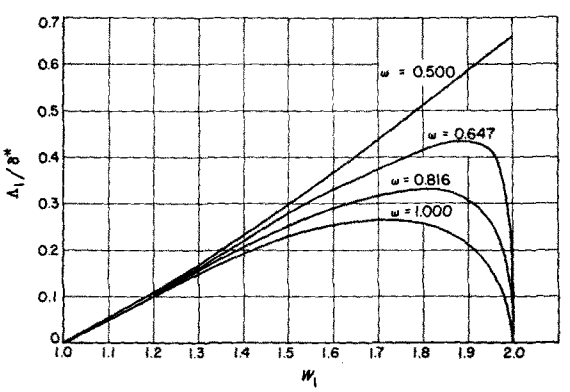

FIG. 3. Navier–Stokes shock thickness as a function of the nondimensional upstream velocity W_1 for different viscosity laws $\mu \sim T^\omega$.

[3] R. Becker, Z. Physik **8**, 321 (1922).

[4] H. W. Liepmann and A. Roshko, *Elements of Gasdynamics* (John Wiley & Sons, Inc., New York 1957), p. 57.

TABLE I. Comparison of Λ_1/δ^* according to Eq. (2.7) with Λ_1/δ_m as given by Gilbarg and Paolucci (G–P).

	$\omega = 1/2$		$\omega = 0.647$		$\omega = 0.816$		$\omega = 1$	
M_1	Eq. (2.7)	G–P	Eq. (2.7)	G–P	Eq. (2.7)	G–P	Eq. (2.7)	G–P
1.2	0.073	0.070	0.072	0.068	0.071	0.067	0.070	0.067
1.4	0.142	0.136	0.137	0.132	0.133	0.128	0.127	0.122
1.7	0.231	0.222	0.219	0.210	0.205	0.199	0.191	0.187
2.0	0.305	0.292	0.281	0.270	0.255	0.248	0.230	0.224
2.5	0.396	0.381	0.350	0.344	0.304	0.303	0.261	0.264
3.0	0.459	0.437	0.391	0.377	0.324	0.314	0.265	0.261
4.0	0.535	...	0.425	0.410	0.327	...	0.245	...

indicates that the Navier–Stokes approximation may be valid up to the maximum-stress point; this tentative conclusion will be further strengthened below (Sec. II D). Incidentally, Eq. (2.1d) shows that the maximum of the entropy coincides with the maximum of τ. Hence τ and S both have a maximum at the point in the shock layer where $W = (W_1W_2)^{\frac{1}{2}} = 1$. By similar simple manipulation, one can show that the maximum value of τu, and therefore also of q, occurs for $W = \frac{1}{2}(W_1 + W_2)$.

C. Shock Thickness

The results of Sec. II B suggest the definition of a shock thickness based on the maximum stress

$$\delta^* = (u_1 - u_2)\mu^*/\tau^*. \tag{2.6}$$

δ^* is closely related to the often used "maximum slope thickness," δ_m, say. Indeed, it is easy to derive a relation between δ^* as defined in (2.6) and the maximum slope thickness. In particular, one can show $\delta^* > \delta_m$ but that the difference between the two definitions is slight for all reasonable variations of μ with T. Hence δ^* can be compared directly with the maximum slope thickness. For example to compare with the results of Gilbarg and Paolucci,[5] the ratio of Maxwellian mean free path ahead of the shock layer Λ_1 and δ^* is given by

$$\frac{\Lambda_1}{\delta^*} = \frac{12}{5(2\pi)^{\frac{1}{2}}}(1 - \lambda^{-4})^{-\frac{1}{2}} \cdot \frac{W_1(W_1 - 1)}{W_1 + 1}\left(\frac{\lambda^2 - W_1^2}{\lambda^2 - 1}\right)^{\omega - \frac{1}{2}} \tag{2.7}$$

or very nearly by

$$\frac{\Lambda_1}{\delta^*} = \frac{W_1(W_1 - 1)}{W_1 + 1}\left(\frac{\lambda^2 - W_1^2}{\lambda^2 - 1}\right)^{\omega - \frac{1}{2}};$$

here, ω denotes the exponent in a viscosity–temperature law $\mu \sim T^\omega$. Equation (2.7) shows explicitly the dependence of Λ_1/δ^* on ω, in particular that

$$\Lambda_1/\delta^* \to 0 \quad \text{or} \quad \infty$$

depending on $\omega \gtrless \frac{1}{2}$. This result has, of course, been noted before[6] and demonstrates once more the sensitivity of the shock layer to $\mu(T)$ or the assumed molecular-force model.

Figure 3 shows Λ_1/δ^* as a function of W_1 according to Eq. (2.7). The comparison with the exact computations of Gilbarg and Paolucci[5] are shown in Table I; the agreement is evidently as good as can be hoped for.

Other and possibly more useful relations for δ^* can be obtained, e.g., for a monatomic gas

$$R_e^* \equiv \delta^* a^* \rho^*/\mu^* \to 5$$

for infinite shock strength.

However, we will show that the maximum stress (or maximum slope) thickness will be nearly correctly given for all shock strengths by the Navier–Stokes equations and consequently an experimental determination of δ_m is of little use in deciding the value of any particular approximation!

D. Expected Range of Applicability of the Navier–Stokes Approximation

The ratio τ/p is a characteristic parameter of the problem which can be interpreted as a dimensionless measure for the magnitude of the gradients in the variables of state in the shock layer. τ/p is the expansion parameter in the Chapman–Enskog procedure and this method of approximation gives $\tau/p \ll 1$ as a sufficient (but not necessary!) condition for the validity of the Navier–Stokes approximation. Hence, as long as τ/p is small, the Navier–Stokes equations must apply (at least in a monatomic gas).

On the other hand, for a monatomic gas τ/p is easily bounded from kinetic theory by noting that both τ and p are related to the second moments $\overline{\rho c_i c_j}$ of the molecular distribution function $f(c)$ by

[5] D. Gilbarg and D. Paolucci, J. Rat. Mech. Anal. **2**, 617 (1953).

[6] M. Morduchow and P. A. Libby, J. Aeronaut. Sci. **16**, 674 (1949).

$$p = \tfrac{1}{3}\rho(\overline{c_1^2} + 2\overline{c_2^2}), \qquad \tau = p - \rho\overline{c_1^2},$$

so that

$$\left|\frac{\tau}{p}\right| = \left|\frac{2(\overline{c_1^2} - \overline{c_2^2})}{\overline{c_1^2} + 2\overline{c_2^2}}\right| < 2. \tag{2.8}$$

Hence, τ/p cannot exceed 2 and, in fact, should be considerably less for any reasonable distribution function. Now τ/p for the Navier–Stokes solution is easily obtained by manipulating Eq. (2.1b):

$$\frac{\tau}{p} = -\lambda^2 \frac{(W_1 - W)(W - W_2)}{\lambda^2 - W^2}. \tag{2.9}$$

The relation is plotted in Fig. 4 and its general behavior shows that τ/p reaches its maximum value upstream of the maximum stress point. Indeed two results from (2.9) are noteworthy:

At the sonic point $W = 1$,

$$|\tau/p|^* = [\lambda^2/(\lambda^2 - 1)](W_1 - 1)(1 - W_2);$$

for an infinitely strong shock $W_1 = \lambda$, $W_2 = 1/\lambda$, hence

$$|\tau/p|^* \to \lambda(\lambda - 1)/(\lambda + 1). \tag{2.10}$$

Furthermore, the largest possible value of τ/p occurs for $W_1 = \lambda$ and $W \to W_1$, i.e., near the low-pressure (upstream) end of the shock layer, and has the value

$$|\tau/p|_{\max} = \tfrac{1}{2}(\lambda^2 - 1). \tag{2.11}$$

In particular, for a monatomic gas (2.10) and (2.11) show that the value of τ/p at the point of maximum stress never gets larger than 2/3, while upstream the maximum value of τ/p reaches 3/2. Thus, we conclude that the critical region for failure of the Navier–Stokes approximation is the part of the shock layer upstream of the maximum stress point.

The first-order distribution function of the Chapman–Enskog procedure [cf. Eq. (3.7)], from which the Navier–Stokes equations result, involves terms proportional to τ/p and to q/p. This means (with $q = \tau u$) that both τ/p and $(\tau/p)M$, i.e., τ/p multiplied by the local Mach number, enter and both should be small. Thus, the difference between the subsonic and supersonic region within the shock layer, i.e., the region upstream and downstream of the maximum stress point, is again emphasized. Downstream of $W = 1$, $M < 1$ and, hence, if τ/p is small $(\tau/p)M$ is small *a fortiori*. Upstream of the point $W = 1$, $M > 1$ and, hence, $(\tau/p)M$, which becomes large even faster than τ/p, dominates the approximation. Thus our tentative conclusion, that if the Navier–Stokes approximation fails it will do so in the upstream region, is emphasized even more.

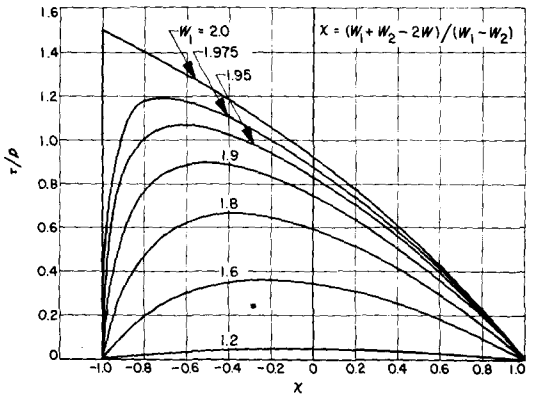

FIG. 4. The Navier–Stokes value of the parameter τ/p within shock as a function of velocity.

Actually, of course, $(\tau/p)M \to \infty$ when $\tau/p \to 3/2$ and the Chapman–Enskog method is certainly inapplicable in this region of the layer.

III. AN INTERPRETATION OF THE B-G-K MODEL FOR COLLISIONS

The questions raised in the last section about the validity of the Navier–Stokes equations in the study of shock structure can only be answered by a more general kinetic theory, and for this purpose we use here the Boltzmann equation with the collision model suggested by Bhatnagar, Gross, and Krook.[7] It is worthwhile first to consider briefly what this model implies: a more detailed discussion will be found in reference 8.

The Boltzmann equation for a monatomic gas with no external forces can very generally be written in the form

$$\left(\frac{\partial}{\partial t} + \mathbf{v}\cdot\frac{\partial}{\partial \mathbf{x}}\right) f(\mathbf{x}, t; \mathbf{v}) = \mathcal{G}(f) - f\mathcal{L}(f), \tag{3.1}$$

where f is the number density of molecules in physical ($\mathbf{x}$) and velocity ($\mathbf{v}$) space, and $\mathcal{G}(f)$ and $\mathcal{L}(f)$ are well-known nonlinear integral operators on f giving, respectively, the number of molecules gained and lost per unit volume and unit time at $(\mathbf{x}, t; \mathbf{v})$. These operators (which are what make the Boltzmann equation difficult) contain the intermolecular force field, which ought to be derivable from other "first principles"; but, in practice, one is compelled to postulate various models for it, of the kind discussed by Chapman and Cowling,[9] e.g., and choose from

[7] P. L. Bhatnagar, E. P. Gross, and M. Krook, Phys. Rev. 94, 511 (1954).

[8] R. Narasimha, Ph.D. thesis, California Institute of Technology, Pasadena, California (1961).

[9] S. Chapman and T. G. Cowling, *The Mathematical Theory of Non-Uniform Gases* (Cambridge University Press, New York, 1960).

among them the one that best fits some measured bulk properties of the gas (e.g., the viscosity).

The basic idea behind the B–G–K model is that a detailed prescription of the force field is much too fine for many purposes, and that it may be more useful to postulate, at a grosser level, a statistical model for the whole scattering process. Among the simplest of these is the one we shall use here, namely,

$$\mathfrak{L}(f) = An, \qquad \mathcal{G}(f) = AnF = An^2(\beta/\pi)^{\frac{3}{2}} \cdot \exp\,[-\beta(\mathbf{v}-\mathbf{u})^2], \tag{3.2}$$

where n, $\mathbf{u}$, and $T = \frac{1}{2}R\beta$ are, respectively, the local number density, gas velocity, and temperature, and can be written down as simple moments of f:

$$n = \int f\, D\mathbf{v}, \qquad n\mathbf{u} = \int f\mathbf{v}\, D\mathbf{v}, \qquad 2RT = \frac{1}{\beta} = \frac{2}{3n}\int m(\mathbf{v}-\mathbf{u})^2 f\, D\mathbf{v}. \tag{3.2a}$$

(Here, m is the mass of the molecule and R is the gas constant.) The number A is a free parameter which in general may depend on the state of the gas. An even simpler version of (3.2), which has been used quite often, takes $An = \bar{\nu} = \text{const}$ for a given flow; the model in this case may properly be called a "single-relaxation-time" model, but would be too simple for any flow with wide variations in the state of the gas, like those that occur in a shock wave.

The model (3.2) replaces the "exact" collision integrals of Boltzmann by terms containing only a few of the lowest moments of f; but these moments are not known beforehand, and the resulting equation

$$\partial f/\partial t + \mathbf{v}\cdot\partial f/\partial \mathbf{x} = An(F - f) \tag{3.3}$$

is still a nonlinear integro-differential equation. It is easy to see that the terms (3.2) possess the same five collisional invariants m, $m\mathbf{v}$, and mv^2 as the exact integrals; hence, (3.3) yields, on the integration with these invariants, the true macroscopic equations of motion for a monatomic gas

$$\begin{aligned} d\rho/dt + \rho\,\partial u_i/\partial x_i &= 0, \\ \rho\, du_i/dt &= -(\partial/\partial x_i)p_{ij}, \\ \rho(d/dt)(\tfrac{1}{2}u^2 + 3p/2\rho) &= -(\partial/\partial x_i)(p_{ij}u_j + q_i), \end{aligned} \tag{3.4}$$

where $p_{ij} = \overline{\rho c_i c_j}$ is the pressure tensor and $q_i = \overline{\rho c^2 c_i}$ is the heat-flow vector.

There are many ways of looking at the B–G–K model, but the following seems to bring it closest to the Boltzmann equation. As pointed out by Kogan,[10] we can recognize the loss term as having the form expected for Maxwell molecules (force $\propto r^{-5}$), for which the integral

$$\mathfrak{L}(f) = \int f(\mathbf{w})gI\, d\Omega\, D\mathbf{w}$$

is just proportional to the number density, as gI is independent of $\mathbf{w}$. (g is the relative velocity between two colliding molecules and I the cross section for scattering into the solid angle $d\Omega$.) We call the constant of proportionality A, noting that we will have to use a cutoff in the scattering angle to make the integral finite. The total number of molecules "lost" (which is twice the number of collisions) is just the integral of $f\mathfrak{L}(f)$ over all velocities, and so is An^2. For a gas of hard spheres in equilibrium this number is $n\bar{c}/l$, where $\bar{c}$ is the mean thermal speed and l is a mean free path. Thus, putting

$$A = \bar{c}/nl \tag{3.5}$$

matches the number of collisions.

The gain integral is more difficult to handle. It is a well-known result in kinetic theory that two colliding rigid spheres scatter isotropically in their center-of-mass frame; if this result can be extended to any number of colliding spheres, the scattering would be isotropic in a frame moving with the local gas velocity $\mathbf{u}$, i.e., $\mathcal{G}(f)$ would only be a function of the peculiar speed $c = |\mathbf{v} - \mathbf{u}|$. As a first approximation, we may take this function of c to be universal in form independent of f; then, the requirement that the collision integral should vanish when f is Maxwellian suggests that $\mathcal{G} \sim F(c)$, and leads to (3.2).

The assumption that $\mathcal{G}$ is a universal function (with five free parameters, of course) seems to be the strongest underlying the model. It can be looked upon as an extension of the familiar assumption of diffuse reflection at a surface to collisions within the gas itself, the emerging molecules having accommodated themselves instantaneously to the local state of the gas. The relaxation time for the gas as a whole is still not zero, because only a fraction of the molecules present at $\mathbf{x}$ are taking part in collisions at any given instant.

The B–G–K model is thus a rough representation of the collision integrals, inspired partly by Maxwell molecules and partly by rigid spheres—an inconsistency which we hope is not serious, at least qualitatively. To see its implications a bit further, one can apply the conventional Chapman–Enskog procedure to the model. If we nondimensionalize (3.3), using some scale L of the flow as a character-

[10] M. N. Kogan, Prikl. Mat. Mekh. **22**, 425 (1958); see also reference 8.

istic length and some speed V as a characteristic velocity, we get

$$\frac{\partial f}{\partial t} + \mathbf{v}\cdot\frac{\partial f}{\partial \mathbf{x}} = \alpha(F - f), \qquad \alpha = \frac{AnL}{V}. \tag{3.6}$$

If $V \sim \bar{c}$, α is just a multiple of the inverse Knudsen number; if $V \sim u$ (which is more appropriate especially at high Mach numbers), $\alpha \sim L/M\Lambda$. The Chapman–Enskog procedure consists of expanding f in powers of α_0^{-1}, where α_0 is a typical value of α and is very large:

$$f = f^{(0)} + \alpha_0^{-1}f^{(1)} + \alpha_0^{-2}f^{(2)} + \cdots .$$

The solution is simply

$$f^{(0)} = F, \qquad f^{(n)} = -\frac{\alpha_0}{\alpha}\left(\frac{\partial}{\partial t} + \mathbf{v}\cdot\frac{\partial}{\partial \mathbf{x}}\right)f^{(n-1)}, \qquad n \geq 1.$$

Substitution of the zeroth-order term into the equations of motion (3.4) yields the Eulerian gas-dynamics equations. The first-order term is easily evaluated, again using (3.4), to be

$$f^{(1)} = \frac{\alpha_0 L}{\alpha V} F\left[\frac{c_k}{\beta}\frac{\partial \beta}{\partial x_k}\left(\beta c^2 - \frac{5}{2}\right) - 2\beta\frac{\partial u_k}{\partial x_l}(c_k c_l - \tfrac{1}{3}c^2\,\delta_{kl})\right] + O\left(\frac{\Lambda}{L\alpha_0}\right),$$

which is very similar to the Chapman–Enskog solution of the full Boltzmann equation. When the pressure tensor and heat flux are worked out, we can write $f^{(1)}$ as

$$f^{(1)} = \alpha_0 F[(2\beta/p)q_k c_k(\tfrac{2}{5}\beta c^2 - 1) - (\beta\tau_{kl}/p)c_k c_l] \tag{3.7}$$

and obtain the familiar transport parameters as

$$\mu = \frac{1}{2A\beta m}, \quad \mu' = -\frac{1}{3A\beta m}, \quad k = \frac{5R}{4A\beta m}, \tag{3.8}$$

where μ and μ' are the ordinary and second viscosity coefficients, and k is the thermal conductivity. Obviously, the Stokesian relation $\kappa = 3\mu' + 2\mu = 0$ is satisfied, as it is in the exact kinetic theory. But

$$\mathrm{Pr} = \mu c_p/k = 1, \quad \text{or} \quad \tilde{\mathrm{Pr}} = 4/3,$$

whereas the correct value for monatomic gases is very nearly $\mathrm{Pr} = \frac{2}{3}$. As the measured viscosity of gases is a function only of the temperature, so [from (3.8)] should A be. In fact, A can be determined for any gas from its viscosity (e.g., for Maxwell molecules A is a constant, for rigid spheres $A \sim T^{\frac{1}{2}}$). This will automatically give the right temperature dependence for k, too, though the numerical values will not be correct because of the wrong Prandtl number.

In the study of shock structure it has been known since the work of Thomas[11] that the variation of transport parameters with temperature is an essential feature which cannot be ignored; here we take account of it by making A a suitable function of temperature (see Sec. IV B). The fact that the Prandtl number is rather different from the true value should, however, make no qualitative difference to our conclusions.

The second-order term $f^{(2)}$ leads similarly to Burnett-like expressions for the stresses and heat flow, but their value in understanding shock structure is doubtful. In any case, the model we are using reproduces all the essential features of the Boltzmann equation near the continuum limit $\alpha \to \infty$, $f \to F$. Free-molecular flow corresponds to the opposite limit $\alpha = 0$ where, of course, the collision model is irrelevant. There are several solutions for small α using the model[12,13], but there is no exact kinetic-theory calculation with which to compare these results. So here one has to rely on experiments, and, though the evidence is not conclusive, calculations made for nearly free-molecular flow through an orifice at very large pressure ratios have shown encouraging agreement with measurements,[13,14] and this gives one confidence that the model faithfully imitates the Boltzmann equation throughout the whole Knudsen number range.

IV. B-G-K MODEL APPLIED TO SHOCK STRUCTURE

A. Formulation of the Problem

It is well known that the transition in flow quantities across a shock occurs in a few mean paths; and the fundamental problem in studies of shock structure is to define precisely the conditions under which one can use the Navier–Stokes or other continuum equations to describe this transition, and to indicate what deviations should be expected when those conditions do not obtain. We have sought to show in the last section that the B–G–K model is sufficiently general to answer this question at least qualitatively; for a complete quantitative answer, one has to tackle the full Boltzmann equation, and this still does not seem possible.

Actually, it is not possible to solve even the model equation exactly, and here we use an iteration to get approximate solutions. The scheme is quite general and can be applied to any problem, but we just consider the plane normal shock (Fig. 1). We

[11] L. H. Thomas, J. Chem. Phys. **12**, 449 (1944).
[12] D. R. Willis, Princeton University Aeronautics Engineering Dept. 442 (1958).
[13] R. Narasimha, J. Fluid Mech. **10**, 371 (1961).
[14] H. W. Liepmann, J. Fluid Mech. **10**, 65 (1961).

can then write (3.3) as

$$v_x(df/dx) = An(F - f). \tag{4.1}$$

Integrating this formally for $v_x \gtrless 0$, respectively, and imposing the boundary conditions

$$\begin{aligned} f(-\infty\,;\mathbf{v}) &= F_1 = n_1(\beta_1/\pi)^{\frac{3}{2}} \\ &\quad \cdot \exp\left[-\beta_1(\mathbf{v}-\mathbf{u}_1)^2\right], \\ f(+\infty\,;\mathbf{v}) &= F_2 = n_2(\beta_2/\pi)^{\frac{3}{2}} \\ &\quad \cdot \exp\left[-\beta_2(\mathbf{v}-\mathbf{u}_2)^2\right], \end{aligned} \tag{4.2}$$

where the parameters are determined from the Rankine–Hugoniot conditions, we obtain an integral equation for f

$$f(x; v_x > 0) = f_+ = \int_{-\infty}^{x} \frac{AnF}{v_x}\left[\exp\left(-\int_{x'}^{x}\frac{An\,dx''}{v_x}\right)\right]dx', \tag{4.3a}$$

$$f(x; v_x < 0) = f_- = \int_{+\infty}^{x} \frac{AnF}{v_x}\left[\exp\left(-\int_{x'}^{x}\frac{An\,dx''}{v_x}\right)\right]dx', \tag{4.3b}$$

where we have omitted the "complementary-function" solution of (4.1) as the boundaries are at infinity. The integral essentially samples $F(v_x)$ over a distance of order v_x/An, which is actually a kind of free path at velocity v_x. It is seen that if $F(v_x)$ is constant over regions much larger than this, the integral just reproduces it; so, far away from the shock, $f(\mp\infty\,;\mathbf{v}) = F_{1,2}(\mathbf{v})$, irrespective of the sign of v_x, and the boundary conditions will be satisfied.

The integral equations (4.3) can be solved by iteration: We make a first guess $F^{(0)}(x;\mathbf{v})$ for F, and using this as the "input" evaluate $f = f^{(1)}$; from this we get new values for $n(x)$, $\beta(x)$, and $u(x)$, form the new $F^{(1)}(x;\mathbf{v})$ and compute $f = f^{(2)}$. We first tried the discontinuous distribution

$$F^{(0)}(x<0) = F_1, \qquad F^{(0)}(x>0) = F_2,$$

where F_1 and F_2 are obtained from the Rankine–Hugoniot relations across the shock. The first iterate gave an interesting structure to the shock, but could not resolve the infinite slope at $x = 0$.

We next used the Navier–Stokes solution to provide a first guess at $n^{(0)}$, $u^{(0)}$, $\beta^{(0)}$, in $F^{(0)}$, and this turned out to be very satisfactory; The rest of the results here are all based on this scheme. First, the Navier–Stokes equations were solved for the Sutherland viscosity law and, to be consistent with the B–G–K model, for Pr = 1. The n, β, and u so obtained were then used in F to generate $f^{(1)}$, etc. The details of the computations, which were fairly involved, are described in Sec. IV B.

This method is particularly suited to the use of the B–G–K model as only the first few moments are needed for computing the collisions, and not the whole distribution. It should be emphasized that, because of this, the higher iterates we obtain have nothing in common with the Burnett and other similar higher-continuum approximations of kinetic theory; The iteration is *not* carried out on the Chapman–Enskog distribution. In fact, the form of f in our iteration never really changes, being always given by (4.3) which is obviously unlike the Chapman–Enskog or Burnett expressions; only the parameters in f change. At each stage in the iteration, (4.3) gives an approximate representation of f which is uniformly valid in velocity space, which cannot be said for the so-called "higher approximations."

Nevertheless, these "higher approximations" are contained in (4.3). To see how, define for convenience a new variable

$$\xi = \int_0^x An\,dx';$$

then, we can write (4.3a) for $v_x > 0$ [and also (4.3b) similarly, of course] as

$$f(\xi; v_x > 0) = \int_{-\infty}^{\xi} \frac{F(\xi';\mathbf{v})}{v_x}\exp\left[-\frac{(\xi-\xi')}{v_x}\right]d\xi'.$$

Now, if F varies sufficiently slowly in ξ/v_x, i.e., if the free path v_x/An is sufficiently small compared with the distance over which there is a significant change in $F(v_x)$, we can obtain an asymptotic expansion for f in the usual way by expanding F in a Taylor series at ξ, getting

$$f(x; v_x > 0) = F(x) + (v_x/An)(dF/dx) + \cdots,$$

and this is just the simple one-dimensional version of the Chapman–Enskog series discussed in Sec. III, the second term above giving the Navier–Stokes equations, etc. Note that this is an asymptotic series, which, for fixed An (no matter how large), can never be valid for sufficiently large v_x. It is perhaps for lack of appreciation of this fact that the "higher approximations" have usually failed.[15] Of course the difficulty can be avoided by always using the full integral (4.3), but this seems possible only with high-speed computers.

The physical nature of the above iteration is clear. At each stage, the iteration properly samples and weights the input (i.e., the previous iterate), and redistributes the flow quantities accordingly. It was

[15] These and related points will be amplified in a forthcoming paper by R. Narasimha.

shown in Sec. II that the gradients in the Navier–Stokes shock are fairly small (relative to the local mean free path) in the downstream part; hence, here the sampling distance is also quite small, and one expects the Navier–Stokes structure to reproduce itself. Upstream, however, the gradients and sampling distance (for velocities v_x of order u, *which contribute most to the moments*!) are greater, and a larger part of the input is weighted in the iteration, so larger deviations might be expected. If the iteration is convergent, it will finally lead to the true solution, which by definition is properly weighted.

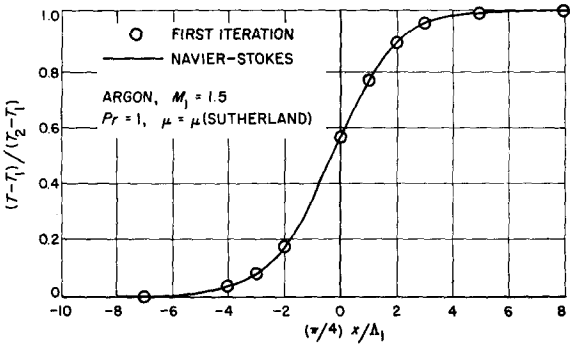

FIG. 6. Temperature profile of a shock at $M_1 = 1.5$.

B. Computations

The computations reported in this paper were made for a monatomic gas with the molecular weight and viscosity of argon but with a (constant) Prandtl number Pr = 1, i.e., the parameter A was taken to be $\frac{1}{2}\mu\beta$ [Eq. (3.8)], μ being the viscosity of argon as fitted to a Sutherland law[16]. Four shock profiles were studied, at $M_1 = 1.5$, 3.0, 5.0, and 10.0, respectively. The assumed flow conditions simulate those in a wind tunnel whose reservoir is at room temperature (296°K), except that the free-stream static temperature T_1 has a minimum limiting value (at $M_1 = 5.0$ and 10.0) of 50°K.

The computations were all programmed on an IBM 7090.[17] The Navier-Stokes profiles were first computed at 1001 points within the shock according to the method advanced by Gilbarg and Paolucci,[5] starting from the saddle-point singularity and with the origin of the physical axis taken at the point of maximum velocity gradient. Each iteration was carried over 30 points, and a third-order polynomial was found to be best suited for interpolation purposes. In computing the moments $u(x)$, $n(x)$, and $T(x)$, using Eq. (3.2a), the infinite limits in both velocity and physical spaces proved to be difficult to handle on the computer. However, two considerable simplifications were accomplished: (1) by using the fact that the Navier–Stokes solution converges rapidly to the Rankine–Hugoniot limits, and (2) by cutting off the integration with respect to v_x at the point where

$$\exp\left[\beta(v_x - u)^2 - \int_{x'}^{x} An\,\frac{dx''}{v_x}\right]$$

is $\leq 10^{-32}$. This is done at no cost as far as computational accuracy is concerned and with great saving in storage and time.

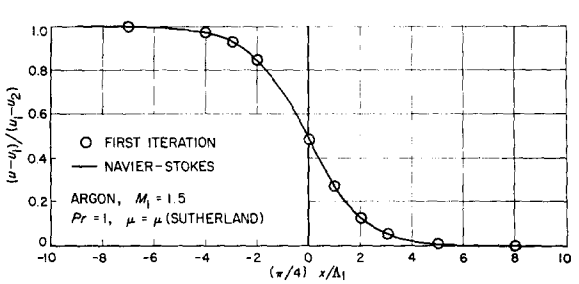

FIG. 5. Velocity profile of a shock at $M_1 = 1.5$.

The computational error introduced in computing u and T is less than $\pm 5 \times 10^{-3}$, while the existence of v_x in the denominator of the integrand leads to a relatively higher error in the computation of the lowest-order moment $n(x)$.

Two features of the iteration, observed in the process of testing for the accuracy and efficiency of the computation, are worth mentioning: (1) the effect of using different orders of accuracy in the integration did not noticeably influence the low-pressure side of the profile, while the high-pressure side seemed more sensitive to any changes in the size of the step of integration; (2) in one instance, the results of an iteration on a less accurate Navier–Stokes solution (computed at 201 points) showed slight but unexpected deviations from the Navier–Stokes on the high-pressure side, but a more refined Navier–Stokes computation (at 1001 points) brought it closer to the iterated result! This gave one considerable confidence in the iteration scheme and the computations. Again, the low-pressure side was not affected in both cases by any of these changes.

The number of iterations performed was limited by the amount of time required or by satisfying the condition imposed by the limits of the computational accuracy. In order to satisfy the latter condition only one iteration was required for $M_1 = 1.5$ (Figs. 5 and 6) and two iterations for $M_1 = 3.0$ (Figs.

[16] *Tables of Thermal Properties of Gases*, National Bureau of Standards Circ. 564 (1955); I. Amdur and E. A. Mason, Phys. Fluids **1**, 370 (1958).

[17] More details about the computations will be found in a forthcoming Jet Propulsion Laboratory report by M. Chahine.

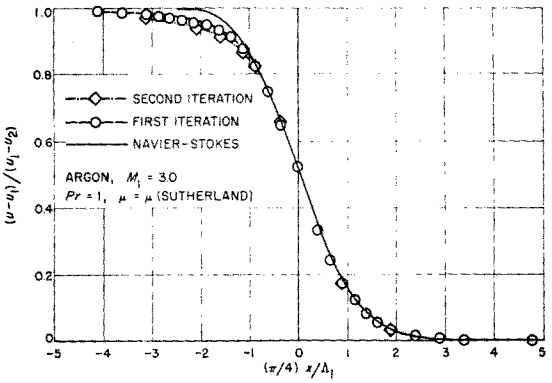

FIG. 7. Velocity profile of a shock at $M_1 = 3.0$.

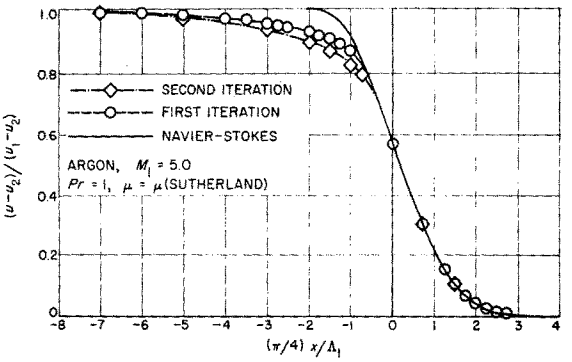

FIG. 9. Velocity profile of a shock at $M_1 = 5.0$.

7 and 8). The convergence was somewhat slower for $M_1 = 5$ and the time limit did not allow more than two iterations (Figs. 9 and 10), but two iterations seemed almost sufficient for $M_1 = 10$ (Figs. 11 and 12).

C. Results

The results of the computations of u and T are shown in Figs. 5 to 12, and some of their more important features are summarized below. It should be pointed out that there has been no relative sliding of these profiles (on the x axis) in any of the figures.

(i) At $M_1 = 1.5$ (Figs. 5 and 6), the iteration reproduces the Navier–Stokes profile almost exactly; the relative change in the temperature, e.g., was less than 10^{-4}. Thus, for weak shocks, the Navier–Stokes solution is in fact very close to the exact kinetic solution.

(ii) At higher Mach numbers (Figs. 7 to 12), the iterations still reproduce the Navier–Stokes solutions very well on the high-pressure side of the shock, up to about the point of maximum slope. On the low-pressure side, however, the iterations show progressively larger deviations from Navier–Stokes as the shocks get stronger, and approach the conditions at infinity more slowly. The shock tends to become thicker and more unsymmetrical than the Navier–Stokes profile (which is itself not symmetric for strong shocks as shown in the recent work of Bush[18]), till for very large M_1 the major part of the shock lies upstream of the maximum slope point.

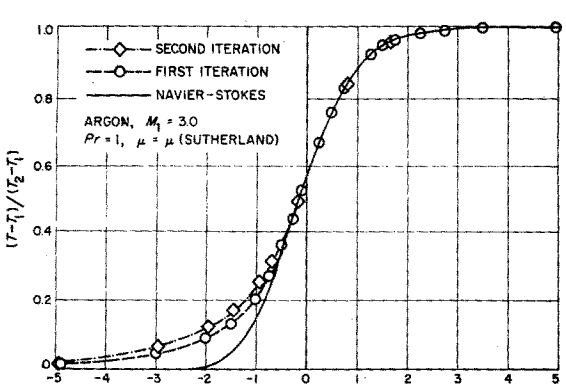

FIG. 8. Temperature profile of a shock at $M_1 = 3.0$.

(iii) As an obvious consequence of the above result, the maximum slope inside the shock, and, hence, any thickness (say δ_m) based on it, is not changed too much from its Navier–Stokes value, even for high M_1: In the present computations, differences in δ_m were hardly noticeable within the numerical uncertainties. A truer measure of the thickness should, however, give weight to the whole structure, and may be defined, following Grad, e.g., based on the area under the profile. (In this definition a "center" of the shock is determined so that the area S between the profile and the corresponding asymptote is equal on either side of the center. The shock thickness is then taken to be $\delta_S = 8S/\Delta$, where Δ is the distance between the asymptotes. It is easy to show that $\delta_S \geq \delta_m$.) Values of δ_S for the Navier–Stokes and the iterated profiles, as also of δ_m, are given in Table II, and it is seen that δ_S increases much more rapidly with M_1 than δ_m. The relation between δ_S and δ_m is itself also a function of M_1.

(iv) The profiles show that the deviations from Navier–Stokes in the velocity (and, hence, also in the density) are much less pronounced than in the temperature—a fact of some significance to measurements of shock structure.

V. DISCUSSION AND CONCLUSIONS

The Navier–Stokes theory of shock structure has had many defenders, and the present work has shown that this faith is to a certain extent justifiable. If one is only interested in obtaining a number for the

[18] W. B. Bush, J. Mécan. (to be published).

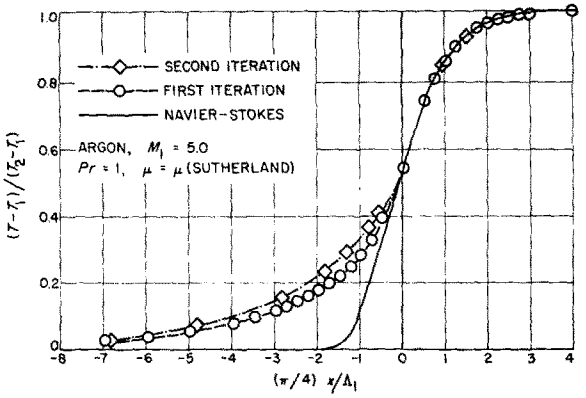

FIG. 10. Temperature profile of a shock at $M_1 = 5.0$.

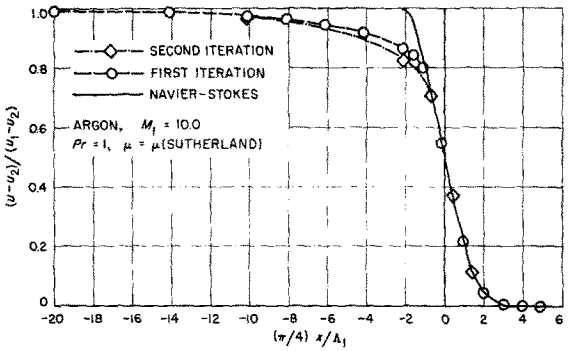

FIG. 11. Velocity profile of a shock at $M_1 = 10.0$.

thickness of the shock based on some flow variable near its steepest part (maximum stress, e.g.), the Navier–Stokes estimate is quite close to the true value: Even for $M_1 = 10$, the difference in maximum slope in velocity was less than 10% in our calculations. However, the Navier–Stokes equations seem inadequate to describe reasonably the details of the structure, especially on the upstream side; here, a more general kinetic theory is essential. The difficulty with the so-called higher-continuum approximations and approaches like the thirteen-moment method is too well known to be detailed here, and is, of course, no criticism of kinetic theory as such.

The inadequacy of the Navier–Stokes equations for handling strong shocks has been widely suspected, but the only alternatives that have been proposed, namely the method of Mott-Smith and its several variants,[19] still lack any rigorous justification. Mott-Smith's results differ from Navier–Stokes for weak shocks, and are certainly wrong at least in this limit. For stronger shocks, Mott-Smith's assumption for f of the bimodal form

$$f = a(x)F_1 + [1 - a(x)]F_2 \qquad (5.1)$$

is usually justified on the grounds that many molecules of the bounding streams will "penetrate" the thin shock. If this were taken seriously, one would have to make superpositions of the two streams with due regard to the sign of v_x, as in Lees' method[20] for handling these problems, instead of taking a linear combination like (5.1); but Lees' method has so far not been successful in tackling shock structure.

Considering the rather arbitrary nature of the Mott-Smith method, it is doubtful whether it can tell us anything about the details of the structure. Thus, the density profile is always symmetric; and the temperature profile shows a maximum inside the shock for $M_1 > 2$. Mott-Smith himself realized that "too much significance cannot be given to the quantitative aspects of these results." However, from the present work, it seems possible that f is bimodal in the upstream (nearly free-molecular) region of the shock, and to the extent that the shock is much more spread out here. Mott-Smith's results may have some local significance; but their value in giving either a "thickness" or the whole structure is questionable.

Unfortunately, the experimental information on shock structure in a monatomic gas at high Mach numbers is not very definite. Sherman[21] has one set of measurements of temperature at $M_1 = 3.70$ in air: These would bear out our conclusions here, qualitatively, except for an unexplained kink in Sherman's Navier–Stokes calculations. The only other experiments are those of Hornig and his collaborators,[22]

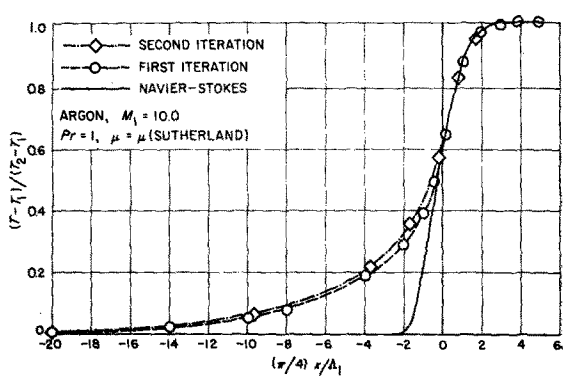

FIG. 12. Temperature profile of a shock at $M_1 = 10.0$.

[19] H. M. Mott-Smith, Phys. Rev. **82**, 885 (1951); P. Rosen, J. Chem. Phys. **22**, 1045 (1954); P. Glansdorff, Phys. Fluids **5**, 371 (1962).

[20] L. Lees, Guggenheim Aeronautical Laboratory, California Institute of Technology, Hypersonic Research Project Memo. 51 (1959); see also L. Lees and C. Y. Liu, Phys. Fluids **5**, 1137 (1962).

[21] F. S. Sherman, NACA Tech. Note 3298 (1955).

[22] K. Hansen, D. F. Hornig, B. Levitt, M. Linzer, and B. F. Myers, in *Rarefied Gas Dynamics*, edited by L. Talbot (Academic Press Inc., New York, 1961), and other references cited there.

TABLE II. Comparison of slope and area thickness[a] of shocks from Navier-Stokes (N-S) and B-G-K solutions.

M_1	Λ_1/δ_m, N-S	Λ_1/δ_s, N-S	Λ_1/δ_s, B-G-K
1.5	5.75	7.49	7.49
3.0	2.85	3.99	6.20
5.0[b]	2.93	3.71	9.55
10.0[b]	3.44	3.88	15.2

[a] All thicknesses are based on the temperature profiles.
[b] Figures for $M_1 = 5.0$ and 10.0 are not strictly comparable with those for $M_1 = 1.5$ and 3.0 because of different free-stream conditions (see Sec. IV B).

who measure the intensity of light reflected from the shock wave at a very nearly glancing angle of incidence. This is an ingenious method which measures essentially the Fourier transform of the density gradient. So far, measurements have not been complete or detailed enough to make a numerical inversion of the transform possible. Instead, a *symmetrical* density profile with one free parameter was fitted to the measured points and the parameter determined by the best fit. Considering the difficulty of the method of measurement, the results are amazingly consistent. However, the results of our computation make it clear that measurements of the density distribution must be accurate to a few percent to differentiate between the Navier–Stokes theory and the kinetic computations. Such an accuracy has not been reached, and we feel that the reported deviation from the Navier–Stokes maximum slope thickness cannot be traced to the failure of the theory as such, but rather to a possible difficulty in using a simple one-parameter family of curves to fit the experiments or to a difference between the real behavior of $\mu = \mu(T)$ and the one used in the theory. Measurement of viscosity at very high temperatures is difficult, to say the least, and indeed Hornig's method may well be used eventually to determine the viscosity of gases from measured shock properties rather than vice versa!

At present, Sherman's hot-wire technique seems to offer more possibilities, since it is more sensitive to the higher moments of the distribution function. We believe that it is very worthwhile to extend Sherman's method and similar measurements capable of detecting the temperature or pressure profiles of strong shock waves.

Theoretical work is being actively continued on many questions raised by the present paper. In particular, we are studying the form of the distribution function and the limits of δ_S for large M_1, and also the analytical nature and limiting behavior of the integral (4.3).

ACKNOWLEDGMENTS

Helpful discussions with Dr. J. D. Cole during the early part of this work are gratefully acknowledged.

The work is the combined result of efforts started from different angles by the authors and made possible by the support of the National Aeronautics and Space Administration (Contract No. NAS7-100, and Research Grant NsG-40-60) and the Office of Naval Research [Contract N-onr 220 (21)].